Desalination and Water Treatment
www.deswater.com

doi: 10.5004/dwt.2018.22771

122 (2018) 176–191
August

Enhanced adsorption of Cu^{2+}, Ni^{2+}, Cd^{2+} and Zn^{2+} ions onto physico-chemically modified agricultural waste: kinetic, isotherm and thermodynamic studies

A. Murugesan[a,*], M. Divakaran[a], P. Senthilkumar[b]

[a]*Department of Chemistry, SSN College of Engineering, Chennai, 603 110, India, Tel. +91 9842881227; emails: murugesana@ssn.edu.in (A. Murugesan), divakaranm@ssn.edu.in (M. Divakaran)*
[b]*Department of Chemical Engineering, SSN College of Engineering, Chennai, 603 110, India, email: senthilkumarp@ssn.edu.in*

Received 23 February 2018; Accepted 30 June 2018

ABSTRACT

Removal of Cu^{2+}, Ni^{2+}, Cd^{2+} and Zn^{2+} ions from single- and multi-component aqueous solution using porous activated carbon (PAC) has been studied. The PAC was prepared by controlling the carbonation temperature of agricultural waste at 500°C and followed by the acid treatment (10 N H_2SO_4). The structural morphology and elemental composition of PAC have been determined by SEM and EDX, respectively. Batch adsorption studies have been carried out to optimize the adsorption parameters such as solution pH, adsorption dosage, initial metal ion concentration and contact time. Metal ions concentrations have been determined by atomic absorption spectrophotometer. Adsorption kinetic equations (pseudo-first order, pseudo-second order, Elovich and intraparticle kinetic models) have been examined to identify the adsorption process and mechanism using adsorption data of contact time. The adsorption kinetic studies show that the adsorption of metal ions onto the PAC follows the second-order kinetic model, and the maximum adsorption capacities of the Cu^{2+}, Ni^{2+}, Cd^{2+} and Zn^{2+} ions were calculated as 57.2, 68.1, 44.2 and 49.3 mg/g, respectively. The adsorption isotherm results suggest that the Freundlich isotherm has been fitted well with experimental data of mono- and multi-layer adsorption. The effect of temperature on the adsorption of (Cu^{2+}, Ni^{2+}, Cd^{2+} and Zn^{2+}) on PAC has been studied at 298, 303, 308, 313 and 318 K, and thermodynamic parameters such as Gibbs free energy change ($\Delta G°$), enthalpy change ($\Delta H°$) and entropy change ($\Delta S°$) have been evaluated. This study shows that the adsorption process of metal ions onto PACs is endothermic, feasible and spontaneous in nature.

Keywords: Adsorbents; Agricultural; Morphology; Multi-component; Thermodynamics

1. Introduction

The toxic heavy metal ions such as Cu^{2+}, Ni^{2+}, Cd^{2+} and Zn^{2+} are well-known pollutants and discharged into the environment in the form of industrial wastewater. Soil and water system have been severely damaged by the heavy metal ion pollutants. These pollutants are non-biodegradable which accumulates in the living organism, thus causing physiological or neurological damage to human and animal even at low concentration. Several methods have been widely applied for the removal of heavy metal ions in the atmosphere. Adsorption methods are widely used for the removal of heavy metal ions because of the simplicity of the experimental procedure in comparison with other methods. The commercial activated carbon has high adsorption capacity and is a potential adsorbent for the removal of metal ions from the industrial wastewater. But it is more expensive and involves high operating costs. Thus, there is a growing demand to find out low-cost, easily available and efficient adsorbent for the adsorption process [1–8].

* Corresponding author.

Presented at the 3rd International Conference on Recent Advancements in Chemical, Environmental and Energy Engineering, 15–16 February, Chennai, India, 2018.

Activated carbon is a well-known material and is used in chemical purification system to remove the heavy metals from gases and aqueous phase liquids. The high surface area, microporosity and charge of carbon materials have highlighted them as ion exchangers, adsorbents, catalysts and separation media. The activated carbon obtained from physico-chemical treatment possesses a wide range of pore volumes, pore sizes and their microporosity is usually well developed which is influenced by the adsorption process [9–16]. In the physical treatment, the carbonaceous material is exposed to a stream of gases at high temperature (less than 500°C) or the carbonaceous material is exposed to activation agents such as hydroxides, zinc chloride, bicarbonates and acids at low temperature (room temperature) as in the chemical treatment. However, the activated carbons are used in the single-component system, but industrial effluents contain a mixture of metals. The competitive adsorption characteristic materials are required to remove the mixture of metal ions from the multi-component system [17–25]. Recently, natural materials of acid-activated carbons have gained particular attention in the adsorption process such as rice husk [26], Psidium guajava [27], sweet potato [28], peanut hull [29], sawdust [30], neem bark [30], coconut shell [31], olive stone [32], cashew nut shell [33] and corncob [34] activated carbons.

Most of the researchers reported the adsorption of heavy metal ions by the single-component system. However, industrial effluents contain the mixture of metal ions and as a result it is necessary to remove two or more metal ions from the effluent simultaneously. Therefore, the study on the simultaneous adsorption of heavy metals from multi-component systems is necessary and most important for the industrial effluent treatment. In the present study, the competitive adsorption of Cu^{2+}, Ni^{2+}, Cd^{2+} and Zn^{2+} ions was investigated from single- and multi-component aqueous system using modified porous activated carbon (PAC). PAC is prepared from a renewable natural (punnai shell) waste material. It was chosen as an adsorbent material for the removal of a mixture of metals due to molecular recognition sites on its surface which is macroporous and inner macropore web that increases adsorption capacity. The dynamic behaviors of the adsorption experimental parameters have been examined and compared the adsorption ability with its raw material. The experimental kinetic and thermodynamic parameters have been evaluated from the batch adsorption experimental data.

2. Experimental setup

2.1. Chemicals

Deionized distilled water and carbonate free water was purchased from Vijaya Scientific chemicals, India. PAC was prepared from natural waste by the procedure adopted by Murugesan et al. [2] in a study. A stock solution of 300 mg/L single- and multi-component metal ions was prepared from their sulfate ($3CdSO_4$ $8H_2O$, $ZnSO_4$ $7H_2O$, $CuSO_4$ $5H_2O$ and $NiSO_4$ $6H_2O$) salts. Experimental standard solutions were diluted from the appropriate amount of stock solution using deionized distilled water. Finally, H_2SO_4, HCl and NaOH were procured from Sigma-Aldrich Chemical, India.

2.2. Synthesis of adsorbents

Punnai shells were collected from Chennai and dried well. Image of punnai shells is shown in Fig. S1. The dried material was heated in a muffle furnace at a high temperature of 400°C to obtain the raw enhanced activated carbon (AC) in ash form. The AC was subjected to acid treatment with H_2SO_4 to obtain porous surface activated carbon for 24 h. It was filtered and washed several times to remove acid, unwanted impurities and dried at 100°C for a day in a hot air oven. Raw material and acid-enhanced activated carbons (Fig. S2) were used for the removal of Cu^{2+}, Ni^{2+}, Cd^{2+} and Zn^{2+} ions from the synthetic corresponding metal ion solution [34].

2.3. Characterization of the adsorbents

The modified activated carbon was characterized by scanning electron microscopy (SEM), energy dispersive X-ray spectrometry (EDX) and particle size analysis. SEM is very useful to determine the surface morphology of the adsorbent and adsorbed material. EDX provides the crystalline and elemental composition information about a material from a few nanometer depths of the material surface via the electron back-scattered detection system attached with a microscope. All the SEM and EDX analyses of the PAC and metal ion adsorbed material was recorded using the Quanta 200 FEG scanning electron microscope at different accelerating voltages with various working distances. The particle size analysis is the technique of resonant mass measurement to detect and accurately count particles in the size range of 50 nm to 5 μm. The particle size analysis of adsorbent samples was performed by Malvern Instruments Particle Size Analyzer (Zetasizer ver. 6.20, MAL 1049897).

2.4. Batch adsorption studies

The adsorption experiment was carried out by preparing various appropriate concentration from the stock solution and stirred for 2 h in a mechanical shaker at 28°C for the removal of Cu^{2+}, Ni^{2+}, Cd^{2+} and Zn^{2+}ions using surface modified activated carbon (PAC) from single-component (stock solution of 300 mg/L of Cu^{2+}, Ni^{2+}, Cd^{2+} and Zn^{2+}) and multi-component aqueous media (mixture of 300 mg/L stock solution of Cu(II), Ni(II), Cd(II), Zn(II)) by using adsorbent dosage of about 50 to 200 mg. The adsorption parameters such as solution pH (7), contact time (120 min), ambient temperature (28°C) and 175 rpm were maintained at their optimum in the adsorption experiment process. Various adsorption parameters (pH, adsorption dosage, contact time and metal ion concentration) were examined to optimize the adsorption process.

$$\% \text{ Removal} = \left[\frac{C_o - C_e}{C_o}\right] \times 100 \quad (1)$$

where C_o and C_e are the initial and equilibrium concentrations (mg/L) of the metal solutions, respectively. All the adsorption experiments were replicated thrice. In the replication process, approximately 5% error was obtained.

2.4.1. Effect of solution pH

The effect of solution pH on adsorption was studied using 20 mL solution of 300 mg/L of single-component (Cu^{2+}, Ni^{2+}, Cd^{2+} and Zn^{2+}) and multi-component metal ions (mixture of 300 mg/L of (MCu(II), MNi(II), MCd(II), MZn(II)) in the pH range 2.0 to 9.0 with an adsorbent dosage of 100 mg. The solutions were stirred well in a mechanical shaker at 175 rpm for 120 min at ambient temperature (28°C). The solutions were then filtered, and the concentration of the metal ion in the filtrate was measured using AA6300 atomic absorption spectrometer (AAS). Zero-point charge of PAC was determined using 50 mL of KNO_3 in the pH range 2–12 (pH was adjusted by adding either 0.1 N HNO_3 or NaOH) with an adsorbent dosage of 100 mg for 48 h at 28°C.

2.4.2. Effect of adsorption dosage

Batch adsorption studies were performed at different adsorbent dosages ranging from 50 to 200 mg with a metal solution of 20 mL containing 300 mg/L of single-component (Cu^{2+}, Ni^{2+}, Cd^{2+} and Zn^{2+}) and multi-component metal ions (mixture of 300 mg/L of (MCu(II), MNi(II), MCd(II), MZn(II)) stirred well in a mechanical shaker at 175 rpm for 120 min at 28°C. The pH of the solution was maintained at 7.0 for metal ions adsorption onto adsorbents, and then the metal ions concentration was measured using AAS.

2.4.3. Effect of contact time

Batch adsorption studies were also carried out at different contact times between 10 and 180 min with an initial concentration of 300 mg/L single- and multi-component metal ions (mixture of 300 mg/L of MCu(II), MNi(II), MCd(II), MZn(II)) solution at pH 7.0. 100 mg of adsorbent dosage was taken and stirred at 175 rpm at 28°C. At regular time intervals between 10 and 180 min, the solutions were taken and the metal ions concentration was measured using AAS.

2.4.4. Effect of initial metal ion concentration

Equilibrium studies were carried out using 100 mg of adsorbent in 20 mL of single-component and the mixture of multi-component metal ions solution at different concentrations ranging from 100 to 500 mg/L. The solution pH of 7 and 120 min contact time was maintained at 28°C. After adsorption process, the filtrate metal ion concentrations were measured using AAS.

2.5. Adsorption kinetics

Adsorption kinetics for the removal of single- and multi-component metal ions was studied using pseudo-first order, pseudo-second order, Elovich and intraparticle diffusion kinetic models [35–39]. The number of single metal ions adsorbed at time t (q_e, mg/g) was calculated using the following equation:

$$q_e = (C_e - C_t) \times \frac{v}{m} \tag{2}$$

where C_t is the concentration of metal ions solution at any time t (mg/L), V is the volume of the solution (L) and m is the mass (g) of the adsorbent.

2.5.1. Pseudo-first order kinetics equation

The pseudo-first-order equation as given by Lagergren relates the adsorption rate to the metal adsorbed amount at time t as follows:

$$\frac{\mathrm{d}q_t}{\mathrm{d}t} = k_1(q_e - q_t) \tag{3}$$

$$\log(q_e - q_t) = \log q_e - k_t \tag{4}$$

where q_e and q_t are the adsorbed amounts of the metal ions at equilibrium and time t, respectively, expressed in mg/g, and k_{ad} is the pseudo-first-order kinetic rate constant, expressed in min^{-1}.

2.5.2. Pseudo-second-order kinetics equation

Ho and McKay's [36] pseudo-second-order kinetic equation is represented below:

$$\frac{dq_t}{dt} = k_2(q_e - q_t)^2 \tag{5}$$

$$\frac{t}{q_t} = \frac{t}{k_2 q_e^{\,2}} + \frac{t}{q_e} \tag{6}$$

where k_2 (g/mg min) is the second-order kinetic rate constant; the differential equation is usually integrated and transformed in its linear form.

2.5.3. Elovich kinetic model

The experimental data were applied to the Elovich kinetic model, which is given in the following equation:

$$q_t = \frac{1}{\beta}\ln(\alpha\beta) + \frac{1}{\beta}\ln(t) \tag{7}$$

where α is the initial adsorption rate constant (mg/(g min)), and the parameter β is related to the extent of the surface coverage activation energy for chemisorptions (g/mg).

2.5.4. Intraparticle diffusion kinetic model

The intraparticle diffusion model is expressed by the following equation suggested by Weber and Morris [39]:

$$q_t = k_p t^{1/2} + C \tag{8}$$

where k_p is the intra-particle diffusion rate constant (mg/g min) and t is the time (min).

2.6. Adsorption isotherms

The non-linear forms of the Langmuir [40] and Freundlich [41] adsorption isotherm models were used to evaluate the adsorption experimental data. The amount of metal adsorbed q_e (mg/g) was determined by using the following mass balance relationship:

$$q_e = (C_o - C_e) \times \frac{V}{m} \tag{9}$$

where V is the volume of the solution (L); m is the mass (g) of the adsorbent.

2.6.1. Langmuir isotherm model

The Langmuir isotherm model is commonly used for adsorption on a completely homogeneous surface, with the interaction between the adsorbent and adsorbate molecules. The interaction between the adsorbed molecules is negligible. This model assumes uniform adsorption energies onto the surface, and the maximum adsorption depends on the saturation level of the monolayer. The non-linear equation of the Langmuir isotherm model is expressed as follows:

$$q_e = \frac{q_m K_L C_e}{1 + K_L C_e} \tag{10}$$

where C_e is the equilibrium concentration of the metal ions in the solution (mg/L), q_e is the adsorbed value of the metal ion at equilibrium concentration (mg/g), q_m is the maximum adsorption capacity (mg/g) and K_L is the Langmuir binding constant, which is related to the energy of adsorption.

The Langmuir isotherm dimensionless constant of the separation factor or equilibrium parameters (R_L) can be used to predict whether the adsorbents are favorable or unfavorable to the adsorption process.

$$R_L = \frac{1}{1 + bC_0} \tag{11}$$

where b is the Langmuir adsorption equilibrium constant and C_0 is the initial metal ion concentration.

2.6.2. Freundlich isotherm model

The Freundlich isotherm model is related for adsorption on a heterogeneous surface. This model explains multi-layer adsorption process. The model applies to adsorption on heterogeneous surfaces with the interaction between the adsorbed molecules, and the application of the Freundlich equation also suggests that the sorption energy exponentially decreases on completion of the sorption centers of an adsorbent. This isotherm is an empirical equation, which can be employed to describe the heterogeneous systems, and is expressed as follows:

$$q_e = K_f C_e^{1/n} \tag{12}$$

where K_f is the Freundlich constant ((mg/g) (L/mg)$^{1/2}$) which indicates the adsorption capacity and represents the strength of the adsorption bond, and n is the heterogeneity factor which represents the bond distribution. The values of n, between 1 and 10 indicate favorable adsorption.

2.7. Thermodynamic studies

Adsorption studies onto synthesized adsorbents were performed with Cu^{2+}, Ni^{2+}, Cd^{2+} and Zn^{2+}ions at different temperatures (298, 303, 308, 313 and 318 K). Thermodynamic experiments were carried out with 50 mL of the respective initial metal ion concentration, at a constant adsorbent dosage of 2 g/L, and with an optimum pH for a predetermined contact time. The thermodynamic parameters (ΔG, ΔS and ΔH) were evaluated using obtained experimental results [42–44].

The thermodynamic study of the adsorption process is significant for the practical application. The free energy of the adsorption ($\Delta G°$) can be estimated with the equilibrium constant using the following equation:

$$\Delta G° = -RT \ln K_c \tag{13}$$

where K_c is the equilibrium constant (L/g), R is the universal gas constant (8.314 kJ/mol K) and T is the absolute temperature (K).

$$K_c = \frac{C_n}{C_e} \tag{14}$$

where C_n is the equilibrium ion concentration removed from the solution which assumed as adsorbed on the adsorbent (mg/L), C_e is the equilibrium metal ion concentration (mg/L). The plots of $\ln K_c$ vs. $1/T$ are obtained in a straight line and the enthalpy change ($\Delta H°$) and the entropy change ($\Delta S°$) values were obtained from the slopes and intercepts of this plot, respectively. $\Delta H°$ and $\Delta S°$ were derived from the following equations:

$$\Delta G° = \Delta H° - T\Delta S° \tag{15}$$

$$\ln K_c = \frac{\Delta S°}{R} - \frac{\Delta H°}{RT} \tag{16}$$

2.8. Recyclability

Desorption of the metal ions from adsorbents, to regenerate the adsorbent is the most important issue in view of the recyclability of the adsorbents. The metal-treated adsorbents were treated with 50 mL of 0.2 N HCl solution for an hour and the solution was filtered, and the filtrate was evaluated to determine the metal recovery, by the AAS. The acid-washed adsorbent was again washed with water to remove the acid present on the adsorbent surface and was reused for further cycles [34].

3. Results and discussion

3.1. Characterization of the adsorbent

The SEM image of the PAC was taken in order to verify the presence of pores on the surface of the PAC adsorbent. The surface characterization of PAC and the Cu^{2+}, Ni^{2+}, Cd^{2+} and Zn^{2+} ion-adsorbed PAC were determined at randomly selected points of the surface at an accelerating voltage of 30 kV, and a working distance of 50 μm. The SEM images of PAC and single-component (only Ni^{2+} ion) and multi-component (MCu(II), MNi(II), MCd(II), MZn(II) metal ions adsorbed PAC are shown in Figs. 1(a), (c), and (d), respectively. The average pore size of PAC was measured using SEM analysis shown in Fig. 1(b). This SEM image indicates the presence of a macroporous structure, clearly illustrated by fissures and holes. The average pore size in PAC was found to be between 1.76 and 2.29 μm in diameter.

The pore size of the PAC was further confirmed by the particle size analysis. The particle size distribution and statistics graph of the PAC are shown in Fig. 2. The particle size of the PAC was measured and is found to be in the range of 800–2,200 nm. The volume of mean particle size is found to be 1,000 nm. The particle size of the PAC was found to be small when compared with that of the other adsorbents from literature (Table 1). SEM image of PAC (Fig. 1(a)) shows that a large number of macropores occurred on the surface which creates large surface area assembly and promote adsorbent sites. From the SEM and particle size analysis of the PAC, it could be confirmed that more adsorbent sites are present on the surface of the adsorbent. SEM images of metal ion adsorbed PAC with single-component (Fig. 1(c)) (only Ni^{2+} ion) and multi-component (Fig. 1(d)) (mixture of MCu(II), MNi(II), MCd(II), MZn(II)) systems show that the macroporous structure of PAC is completely filled by adsorbate. The result of SEM images of metal ion adsorbed PAC suggests that the single- and multi-component adsorption occurs on the surface of PAC.

The EDX spectra of PAC and the multi-component (MCu(II), MNi(II), MCd(II), MZn(II) ions adsorbed PAC are shown in Figs. 3(a) and (b), respectively. The EDX image of PAC clearly shows peaks corresponding to C, N, O, Si, S and K atoms which indicate the presence of these atoms on the surface of PAC. The EDX image of the multi-component ions adsorbed PAC shows the corresponding metal ion peaks in addition to the others, which confirms the adsorption of metal ions on the surface of PAC. Elemental composition (Table 2) of EDX analysis further confirms the adsorption onto PAC. Exact metal ion concentration and adsorption process were further confirmed by AAS analysis.

3.2. Adsorption behavior of PAC

3.2.1. Effect of solution pH on metal ions adsorption onto PAC

The percentage metal ion removal graph of the effect of pH on adsorption is shown in Fig. 4(a). At lower pH (2), the percentage removal of the metal ions is very less (40%–50% for the single-component system and 13%–16% for the multi-component system) because, in lower pH, a large number of hydrogen ions are present around the adsorption surface which may be attributed to the competition with metal ions. PAC adsorbent was carbonized by concentrated H_2SO_4, which enhanced the Bronsted acid sites on the surface at lower pH. Such a situation strong electrostatic repulsion was introduced between the adsorbent sites

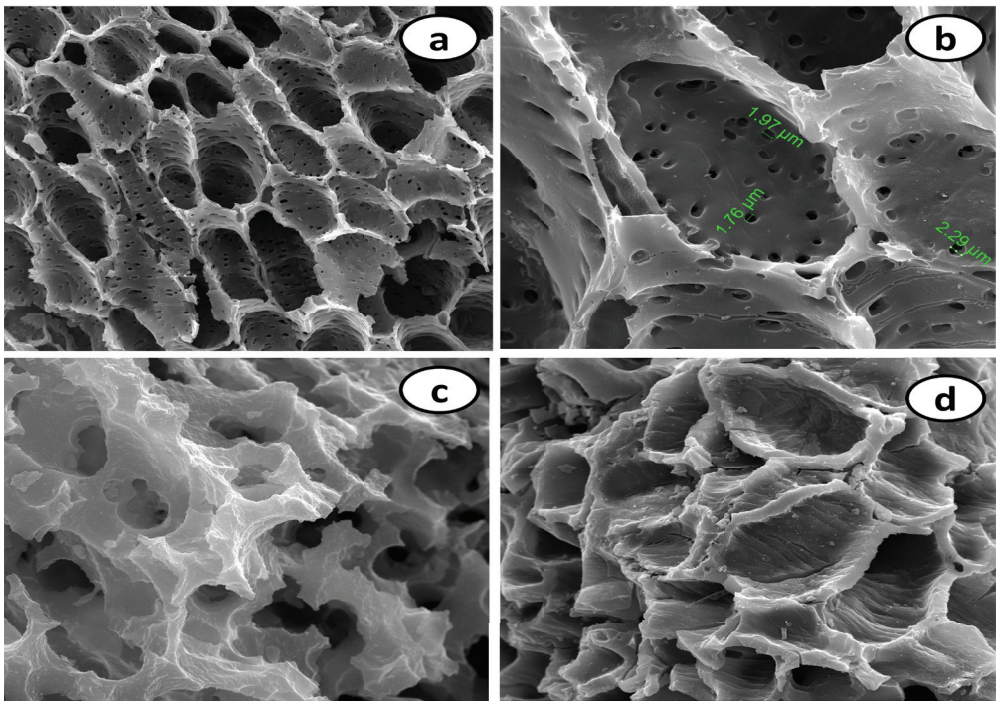

Fig. 1. SEM images of (a) PAC adsorbent, (b) pore size of PAC, (c) single-component (only Ni^{2+} ion) and (d) multi-components (mixture of Cu^{2+}, Ni^{2+}, Cd^{2+} and Zn^{2+} ions) metal ions adsorbed adsorbent, respectively.

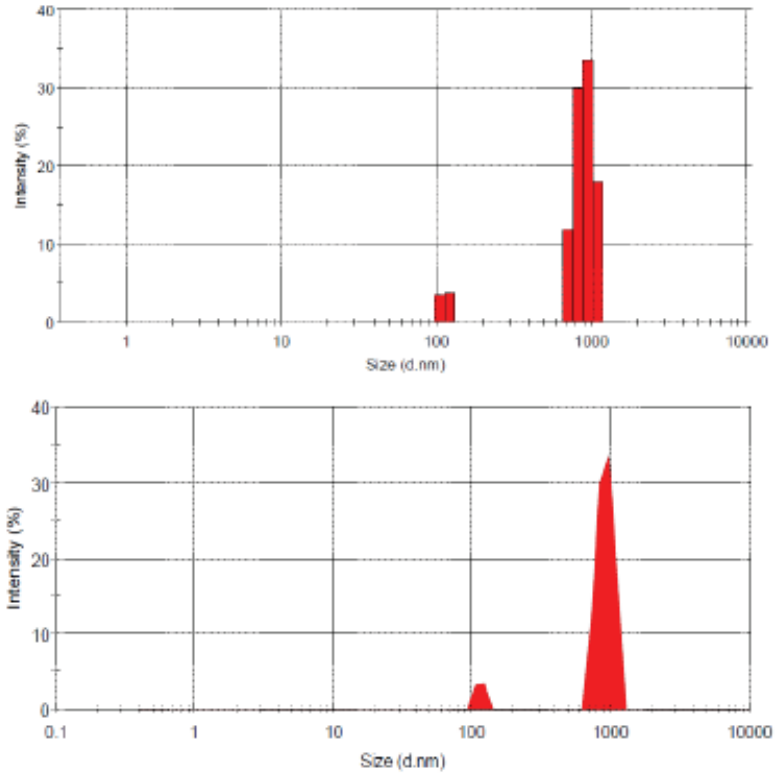

Fig. 2. Particle size distribution and statistics graph of the PAC.

Table 1
Comparison of particle size of various adsorbents for the adsorption of metal ions

Adsorbents	Particle size	References
Palygorskite clay	1–4 μm	[45]
Coconut shell	200–297 μm	[46]
Thiacalix [4] arene-loaded resin	114.80 μm	[47]
Rich husk ash	31.30 μm	[48]
PAC	1,000 nm	Present work

and adsorbate, which enhanced the adsorption capacity at lower pH. With an increase in pH, there is a considerable reduction of H^+ ions, which facilitates the deprotonation of the metal binding sites, which in turn, increases adsorption. At high pH (after pH 7), the metal hydroxides increased gradually, and hence, decreased adsorption is noticed. The percentage removal reaches a maximum value (91%–94% for the single-component system and 26%–34% for the multi-component system) at a pH of approximately 7.0. Hence, in all the batch adsorption experiments, an optimum pH value of 7 has been fixed. Zero point charge (pH_{zpc}) of the PAC is found to be 5.0. At pH > pH_{zpc} (below pH 5), the surface of PAC is positive in nature and adsorbate (metal ion) is also positive in nature which enhanced the electrostatic repulsion between adsorbent and adsorbate. The electrostatic repulsion influenced in the adsorption process and reduced the adsorption capacity below pH_{zpc}. At pH > pH_{zpc} (above

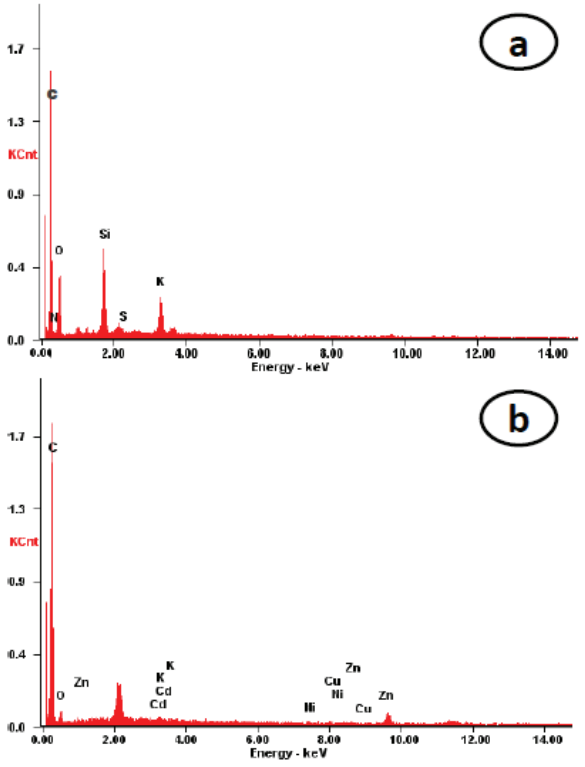

Fig. 3. EDX spectra of (a) PAC and (b) the multi-component (Cu^{2+}, Ni^{2+}, Cd^{2+} and Zn^{2+} ions) metal ions adsorbed PAC, respectively.

pH 5), adsorbent (negative charges) and adsorbate (positive charges) are opposite charges which introduced electrostatic attraction between them, resulting in high adsorption rate on the surface of PAC above pH_{zpc}.

The multi-component system adsorption capacity decreases when compared with the single-component system due to interaction and competition between various metal ions in the solution. The multi-component adsorption studies show that the affinities order of the four divalent metal ions is in the order $Ni^{2+} > Cu^{2+} > Zn^{2+} > Cd^{2+}$. The results suggest that the PAC adsorbent provides a possibility for the selective separation of metal ions from multi-component solutions. The order is similar to the order of the ionic radii of different metal ions studied (Cd^{2+} = 0.95 Å, Zn^{2+} = 0.74 Å, Cu^{2+} = 0.73 Å and Ni^{2+} = 0.69 Å). The smaller the radius of the metal ions, the easier is the diffusion of the metal ion on the adsorption site, and hence, the higher the percentage removal occurred on the surface adsorbent. The adsorption selectivity results show that the PAC adsorbent has good adsorption selectivity and a high capacity for the removal of various metal ions from the mixture.

Table 2
Elemental composition results of EDX analysis

Element	Wt%	
	PAC	Metal ion adsorbed PAC
C	74.21	56.12
N	6.15	3.15
O	18.77	9.77
K	0.88	0.58
Ni	–	12.52
Cu	–	9.24
Zn	–	7.34
Cd	–	5.42

3.2.2. Effect of initial metal ion concentration on metal ions adsorption onto PAC

The experimental results on the effect of initial metal ions concentration on PAC adsorption are shown in Fig. 4(b). According to the figure, the metal ions adsorption is found to be dependent on the initial metal ion concentration. At lower concentrations, metal ions counts are very less compared with adsorbent sites in the solution. Maximum metal ions could interact with the adsorbent sites and facilitate maximum adsorption (98%) in the process. At higher concentration, the percentage of metal ion removal is decreasing due to the constant and saturation of adsorbent sites. After the equilibrium or saturation, more metal ions are left from the adsorbent sites in the solution. So, the percentage removal is decreased.

3.2.3. Effect of adsorbent dose on metal ions adsorption onto PAC

The influence of the adsorbent dose on the removal of single- and multi-component ion onto PAC is shown in Fig. 4(c). The percentage removal of the single- and multi-component

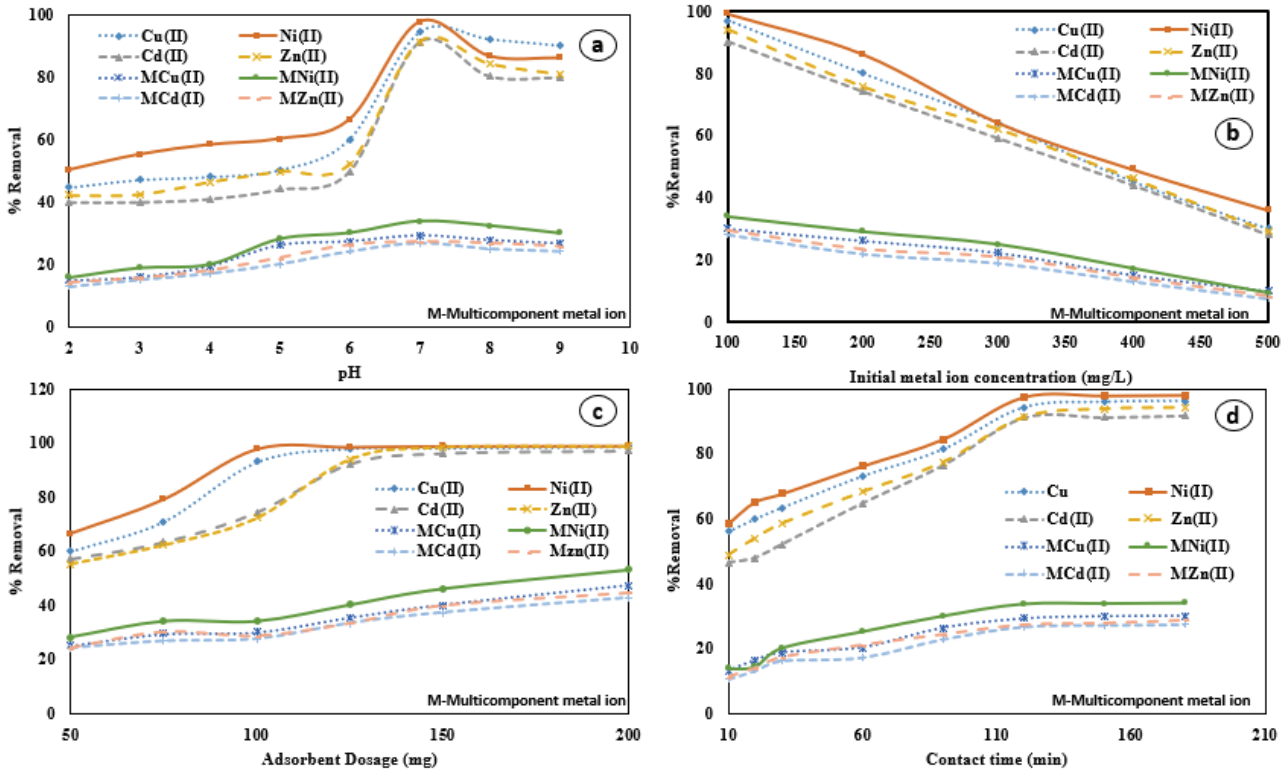

Fig. 4. Effect of (a) pH, (b) initial metal ion concentration, (c) adsorbent dosage and (d) contact time for the adsorption of metal ions onto PAC.

system onto PAC increases from 55% to 99% and 24%–53%, respectively, for an increase in the adsorbent dose from 50 to 200 mg. This is due to an increase in the number of binding sites with an increase in the adsorbent dosage.

In the single-component system, the percentage removal reached saturation after a dose of 100–120 mg because of the maximum adsorption of metal ions, and the fact that the active sites remain vacant on a further increase in the adsorbent dose. In the multi-component system, the percentage removal has not reached saturation after a dose of 150 mg. This is due to the excess of metal ions present in the solution, which may proceed with the adsorption process further with adsorbent sites. This study suggests that the maximum adsorption is attained when all the adsorbent sites are filled or occupied by the metal ions.

3.2.4. Effect of contact time on metal ions adsorption onto PAC

The results of the effect of the contact time on PAC adsorption are shown in Fig. 4(d). The adsorption of Cu^{2+}, Ni^{2+}, Cd^{2+} and Zn^{2+} ions on PAC increases as the contact time is increased and attains equilibrium in 120 min. Initially, the rate of adsorption is higher due to a large number of adsorption sites being available for the uptake of the metal ion from the aqueous medium. After equilibrium, all the sites are occupied and saturated by the metal ions. Beyond this, there is no adsorption noticed. Hence, in the present study, the optimum adsorption occurred is at 120 min and chosen as the equilibrium time.

3.3. Adsorption kinetic studies of PAC

The adsorption process of Cu^{2+}, Ni^{2+}, Cd^{2+} and Zn^{2+} ions onto PAC was investigated using different adsorption kinetic equations, such as the pseudo-first order, pseudo-second order, Elovich and intraparticle diffusion models. The adsorption process and mechanism were verified with experimental kinetic parameters.

3.3.1. Pseudo-first-order kinetic model of PAC

The effect of contact time experimental data of Cu^{2+}, Ni^{2+}, Cd^{2+} and Zn^{2+} ions onto PAC was plotted using pseudo-first-order kinetic equation and are shown in Fig. 5(a). The values of pseudo-first order equilibrium rate constant (k_{ad}), correlation coefficient (R^2) and equilibrium adsorption capacity (q_e) were calculated from the slope and intercept of the plots of ln ($q_e - q_t$) vs. t. The pseudo-first-order kinetic constants are listed in Table 3. The correlation coefficients for the pseudo-first-order kinetic model were found, and they slightly deviated from the pseudo-second-order kinetic model. Moreover, a large difference was observed

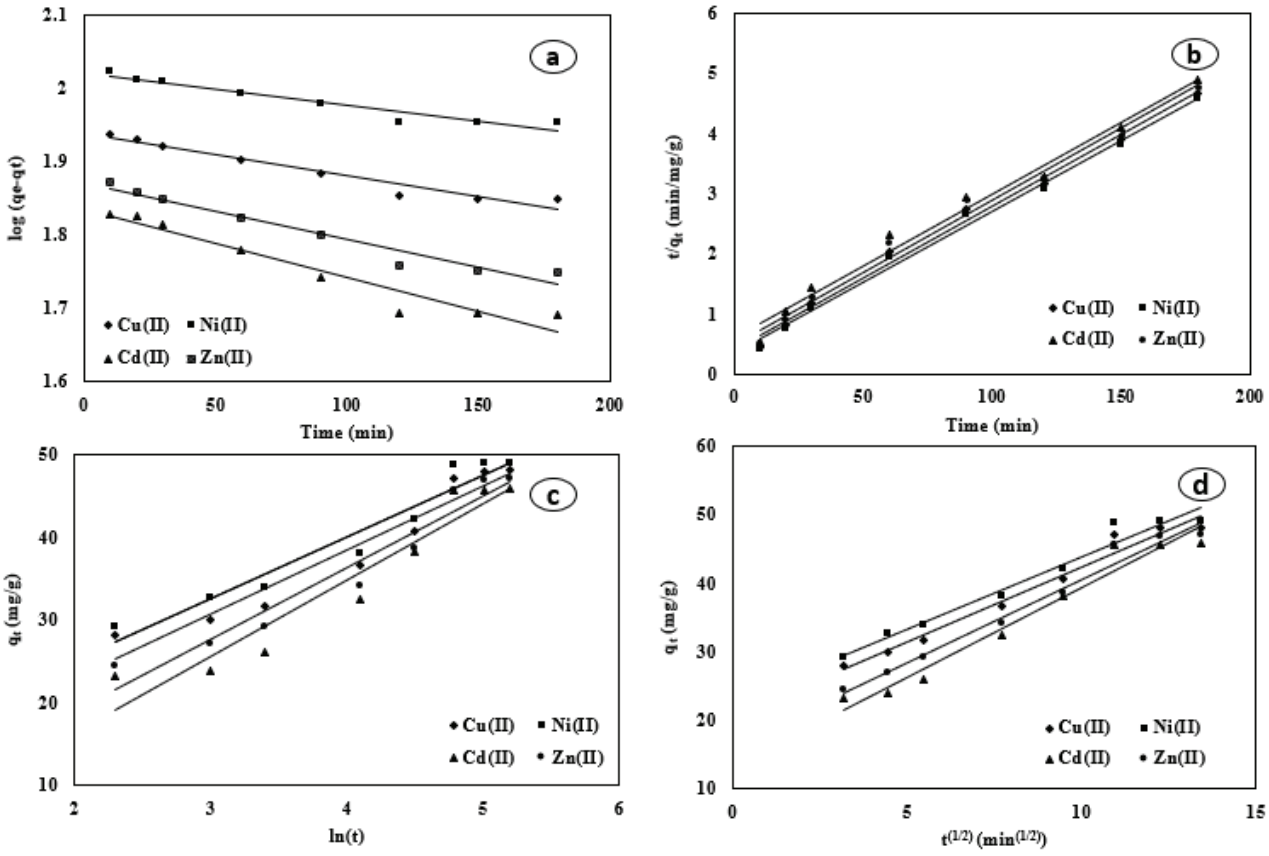

Fig. 5. (a) Pseudo-first order, (b) pseudo-second order, (c) Elovich and (d) intraparticle diffusion kinetic models for adsorption of metal ions onto PAC.

Table 3
Kinetic model statistical parameters for Cu^{2+}, Ni^{2+}, Cd^{2+} and Zn^{2+} adsorption of PAC

Kinetic model	Parameters	Metal ions solution (100 mg/L)			
		Cu^{2+} ion	Ni^{2+} ion	Cd^{2+} ion	Zn^{2+} ion
Pseudo-first-order kinetic model	k_{ad} (min^{-1})	6×10^{-4}	4×10^{-4}	9×10^{-4}	8×10^{-4}
$\ln(q_e - q_t) = \ln q_e - k_{ad} t$	$q_{e,}$ cal (mg/g)	43.3	52.4	34.2	37.2
	R^2	0.9497	0.9350	0.9363	0.9547
Pseudo-second order kinetic model	K_2 (g/mg min)	1.87×10^{-4}	1.52×10^{-4}	2.14×10^{-4}	2.03×10^{-4}
$\frac{t}{q_t} = \frac{1}{k_2 q_e^2} + \frac{1}{q_e} t$	$q_{e,}$ cal (mg/g)	54.1	64.5	43.3	47.3
	h (mg/g min)	2.44	2.82	1.67	1.97
	$q_{e,}$ exp (mg/g)	57.2	68.1	44.2	49.3
	R^2	0.9907	0.9923	0.9840	0.9873
Elovich kinetic model	α (mg/g.min)	20.09	28.58	11.75	10.62
$q_t = \frac{1}{\beta}\ln(\alpha\beta) + \frac{1}{\beta}\ln(t)$	β (g/mg)	0.1283	0.1329	0.1080	0.1154
	R^2	0.9360	0.9441	0.9194	0.9429
Intraparticle diffusion kinetic model	k_p (mg/g.$min^{1/2}$)	2.19	2.10	2.61	2.43
$mq_t = k_p t^{1/2} + C$	C	20.48	22.81	13.31	16.35
	R^2	0.9744	0.9693	0.9612	0.9784

between the experimental value and the calculated value of equilibrium adsorption capacity. R^2 and q_e values indicate that the pseudo-first-order is poorly fit to the experimental data.

3.3.2. Pseudo-second-order kinetic model of PAC

The pseudo-second-order kinetic equation was applied to Cu^{2+}, Ni^{2+}, Cd^{2+} and Zn^{2+} ions adsorption onto PAC. The values of q_e and q_t were calculated from the adsorption experimental data and results are shown in Fig. 5(b). The k_2, R^2 and q_e values for the pseudo-second-order kinetics were calculated from the plot of t/q_t against t (Fig. 5(b)) and are listed in Table 3. In the straight lines, the obtained correlation coefficients (>0.99) are extremely high. In addition, the calculated equilibrium adsorption capacity values also agree with the experimental values in the pseudo-second-order kinetic model. The R^2 and q_e values of this model suggest that the adsorption data are well fitted by the pseudo-second-order kinetics, and hence, the rate-limiting step of metal ions onto adsorbent may be chemisorption. From this kinetic model, it could be suggested that both adsorbent and adsorbate are influenced in the adsorption process.

3.3.3. Elovich kinetic model of PAC

The Elovich kinetic equation was also applied to metal ions (Cu^{2+}, Ni^{2+}, Cd^{2+} and Zn^{2+}) adsorption onto PAC. The values of q_t and ln (t) were calculated from the adsorption experimental data, and the results are shown in Fig. 5(c). The values of α, β and the correlation coefficient (R^2) were calculated from the slope and intercept of the plot, and the values are listed in Table 3. In the Elovich kinetic plot, the characteristic straight lines deviate slightly more than the pseudo-first and pseudo-second-order kinetic plot, which is confirmed by the correlation coefficient (R^2) values. In this model, initial adsorption rate of the process (for Cu^{2+}, Ni^{2+}, Cd^{2+} and Zn^{2+} ions to be 20.09, 28.58, 11.75 and 10.62 mg/g. min, respectively) was defined from α values. From the high initial adsorption rate, it could be suggested that the metal ion interaction with PAC is a chemisorption process. The surface coverage was also defined from β values which range between 0.1080 and 0.1329 g/mg. Based on this, it could be suggested that surface coverage onto the adsorbent is higher. The result of the kinetic model indicates that the experimental data could be fitted with the Elovich kinetic model.

3.3.4. Intraparticle diffusion kinetic studies of PAC

The intraparticle diffusion kinetic equation was also applied to the present study of Cu^{2+}, Ni^{2+}, $Cd^{2+,}$ and Zn^{2+} ions adsorption onto PAC, and the results are shown in Fig. 5(d). The rate constant (K_p), correlation coefficient (R^2) and C values were derived from the intraparticle diffusion plots and listed in Table 3. The plots of q_t vs. $t^{1/2}$ were a double-linear straight line when compared with the plots of other three kinetic models. If the plot is linear, and if it passes through the origin, intraparticle diffusion will be the sole rate-limiting factor and boundary layer adsorption will lead to chelation in the initial stages. The obtained straight line does not pass through the origin. Therefore, the adsorption process seems to be feasible. The plot (Fig. 5(d)) indicates that more than two stages occurred in the adsorption process. In the first stage, the external surface adsorption is attained, and in the second stage, intraparticle diffusion is observed. Finally, the adsorption equilibrium is obtained after the second stage. The diffusion adsorption mechanism is shown in Fig. 6.

The calculated q_e values of metal ions onto PAC from pseudo-first-order plots deviate from the experimental q_e values. This kinetic model might not be sufficient to

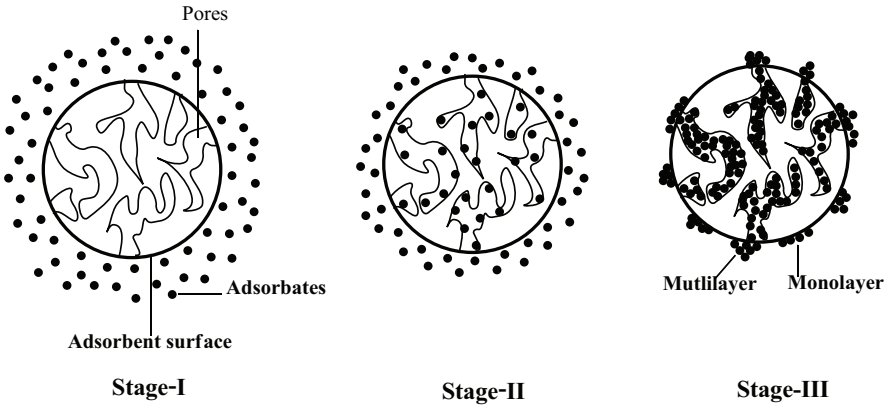

Fig. 6. Diffusion adsorption mechanism of PAC–metal ions system.

describe the adsorption mechanism of the PAC–metal ion interaction. The correlation coefficient (R^2) values were found to be between 0.9350 and 0.9547, which shows that the pseudo-first-order kinetic model moderately fit with the experimental data. The calculated q_e values obtained from the pseudo-second-order kinetic model agree well with the experimental q_e values. The pseudo-second-order kinetic model straight lines and curves fit well with the experimental data than that of the pseudo-first-order kinetic model which is confirmed by R^2 (0.9840–0.9923) values.

In the Elovich plot, α and β values were defined and this explained the rate of initial chemisorption process, the surface coverage of adsorbent and the influence of adsorbate onto the adsorbent system. From the intraparticle diffusion model, the adsorption diffusion mechanism was predicted, and the correlation coefficient values were found to be very lower than the pseudo-first-second kinetic model, viz, between 0.9612 and 0.9784 when compared with other kinetic models. From the above results, it is seen that the pseudo-second-order model is a better fit than other kinetic models. The maximum adsorption capacities of the Cu^{2+}, Ni^{2+}, Cd^{2+} and Zn^{2+} ions were calculated to be 57.2, 68.1, 44.2 and 49.3 mg/g, respectively, using the kinetic equation. Hence, it is suggested that the adsorption of metal ions onto the PAC follows the second-order kinetic model, and the adsorption process and mechanism were derived using all four kinetic models. Reported adsorption capacities of various adsorbents for the removal of Cu^{2+}, Ni^{2+}, Cd^{2+} and Zn^{2+} ions is shown in Table 4. PAC shows higher adsorption capacity when compared with another reported adsorbent. It could be suggested that PAC is a promising adsorbent for the removal of toxic heavy metal ions from industrial wastewater.

3.4. Adsorption isotherm studies of PAC

The non-linear forms of the adsorption isotherm experimental data of PAC for Cu^{2+}, Ni^{2+}, Cd^{2+} and Zn^{2+} ions were evaluated with Langmuir and Freundlich adsorption isotherm models using MATLAB R2009a.

3.4.1. Langmuir isotherm model of PAC

The Langmuir isotherm model is related to monolayer adsorption, and to adsorption on a homogeneous surface. The obtained q_e and C_e experimental data from the study of the effect of initial metal ion concentration were fitted with the non-linear Langmuir adsorption isotherm equation. The curve fits well with the experimental data. The Langmuir constants (K_L), the maximum adsorption capacity (q_m) for the solid-phase loading and the energy constant related to the heat of adsorption were calculated from the non-linear curve. The correlation coefficient (R^2) values were also obtained from the curve. All the constants and parameters of the Langmuir isotherm model are listed in Table 5.

From the Langmuir isotherm model, the maximum adsorption capacities of PAC for Cu^{2+}, Ni^{2+}, Cd^{2+} and Zn^{2+} ions were calculated to be 69.50, 74.33, 54.61 and 60.32 mg/g, respectively. The R_L values between 0 and 1 indicate that the adsorbent–metal system is favorable to the adsorption process. Otherwise, it is unfavorable. The R_L values of the PAC–metal ion system for Langmuir were found to be between 0.11 and 0.74, which suggests that the adsorption process of PAC is favorable. The R_L values further confirm that PAC is a good adsorbent for the removal of heavy metal ions from the single- and multi-component system.

3.4.2. Freundlich isotherm model of PAC

The Freundlich isotherm model is related to multi-layer adsorption, and to adsorption on a heterogeneous surface. The non-linear Freundlich isotherm curve was plotted from PAC adsorption experimental data (q_e and C_e) effect of initial metal ions concentration using the non-linear Freundlich isotherm equation. The isotherm experimental data of PAC also fit well with the Freundlich isotherm equation. The correlation coefficient (R^2), Freundlich constant (K_f) and heterogeneity factor (n) were derived from the non-linear curves. In the present study, the value of n was found to be greater than 1, which indicates that the adsorption of metal ions is a favorable one. All the constants and parameters of the Freundlich isotherm models are listed in Table 5.

The non-linear adsorption isotherm for adsorption of (a) Cu^{2+}, (b) Ni^{2+}, (c) Cd^{2+} and (d) Zn^{2+} ions onto PAC is presented in Fig. 7. The value of R^2 close to 1 indicates that the respective equation fits the experimental data best. The representation of the experimental data by the two models resulted in a non-linear curve with the R^2 values, as tabulated in Table 5. The correlation coefficient value of the Langmuir

Table 4
Comparison of reported and PAC adsorption capacity of various adsorbents for the removal of Cu^{2+}, Ni^{2+}, Cd^{2+} and Zn^{2+} ions

Adsorbent	Modifying agent(s)	Adsorption capacity (mg/g)				References
		Cu^{2+} ion	Ni^{2+} ion	Cd^{2+} ion	Zn^{2+}ion	
Sawdust (*Dalbergia sissoo*)	Sodium hydroxide	–	10.47	–	–	[49]
Sawdust (Oak tree)	Hydrochloric acid	1.39	2.91	–	–	[50]
Sawdust (*Pinus sylvestris*)	Formaldehyde in sulfuric acid	–	–	9.45	–	[51]
Sawdust	Reactive Orange 13	8.07	9.87	17.09	–	[52]
Sawdust (peanut husk)	Sulfuric acid	2.96 3.80	–	–	–	[53]
Jute fibres	Reactive Orange 13	1.32–2.03	1.65–2.36	–	1.48–2.77	[54]
Spent grain	Sodium hydroxide	–	–	17.3	–	[55]
Palm shell activated carbon	(GAC)	1.58	0.13	–	–	[56]
Activated carbons derived from waste olive stones	–	0.15	0.15	–	–	[57]
Activated carbon from almond husk	–	–	30.76	–	–	[58]
Activated carbon from almond husk	Sulfuric acid	–	37.17	–	–	[58]
Acid modified activated carbon (carncob)	Sulfuric acid	–	34.34	–	–	[34]
Acid modified activated carbon (punnai shells)	Sulfuric acid	57.2	68.1	44.2	49.3	Present study

Table 5
Isotherm model statistical parameters for Cu^{2+}, Ni^{2+}, Cd^{2+} and Zn^{2+} adsorption of PAC

Isotherm models	Parameters	Cu^{2+}	Ni^{2+}	Cd^{2+}	Zn^{2+}
Langmuir	q_m	69.50	74.33	54.61	60.32
	K_L	0.0136	0.0161	0.0036	0.0074
	R_L	0.43–0.13	0.38–0.11	0.74–0.58	0.57–0.21
	R^2	0.9498	0.9526	0.9631	0.9694
	SSE	205.7	169.7	123.6	86.54
	RMSE	8.28	7.521	6.874	5.371
Freundlich	K_F	6.728	6.955	2.258	3.829
	n	1.697	1.713	1.177	1.376
	R^2	0.9684	0.9791	0.9966	0.9848
	SSE	87.24	58.9	51.8	42.82
	RMSE	5.393	4.4310	4.378	3.778

isotherm for PAC is low when compared with that of the Freundlich isotherm models. The experimental data fit based on its correlation coefficient values for the Ni^{2+}, Cu^{2+}, Zn^{2+}, Pb^{2+} and Cd^{2+} ions. The adsorption isotherm results clearly suggest that the Freundlich isotherm has a better fit compared with the Langmuir isotherm models and mono- and multi-layer adsorption has also occurred due to the physical and chemical nature on the adsorbent surface.

3.5. Thermodynamic studies of PAC

The effect of temperature on the adsorption of the Cu^{2+}, Ni^{2+}, Cd^{2+} and Zn^{2+} ions onto PAC has been studied at 298, 303, 308, 313 and 318 K, and the results are shown in Fig. 8. The thermodynamic parameters, such as Gibbs' free energy change ($\Delta G°$), enthalpy change ($\Delta H°$) and entropy change ($\Delta S°$) were derived using thermodynamic equations (Eqs. (13)–(16)). $\Delta H°$ and $\Delta S°$ were defined from the slope and the intercept of the plot of $\ln C_e$ vs $1/T$ and $\ln K_c$ vs. $1/T$ (Figs. 9(a) and (b)). The obtained thermodynamic parameters are listed in Table 6. The positive enthalpy changes of thermodynamic values suggest that the adsorption process is endothermic in nature. The negative values of $\Delta S°$ describe the randomness at the PAC–solution interface during adsorption. The Gibbs free energy change increases as the temperature is increased and hence decreased adsorption was noticed. At higher

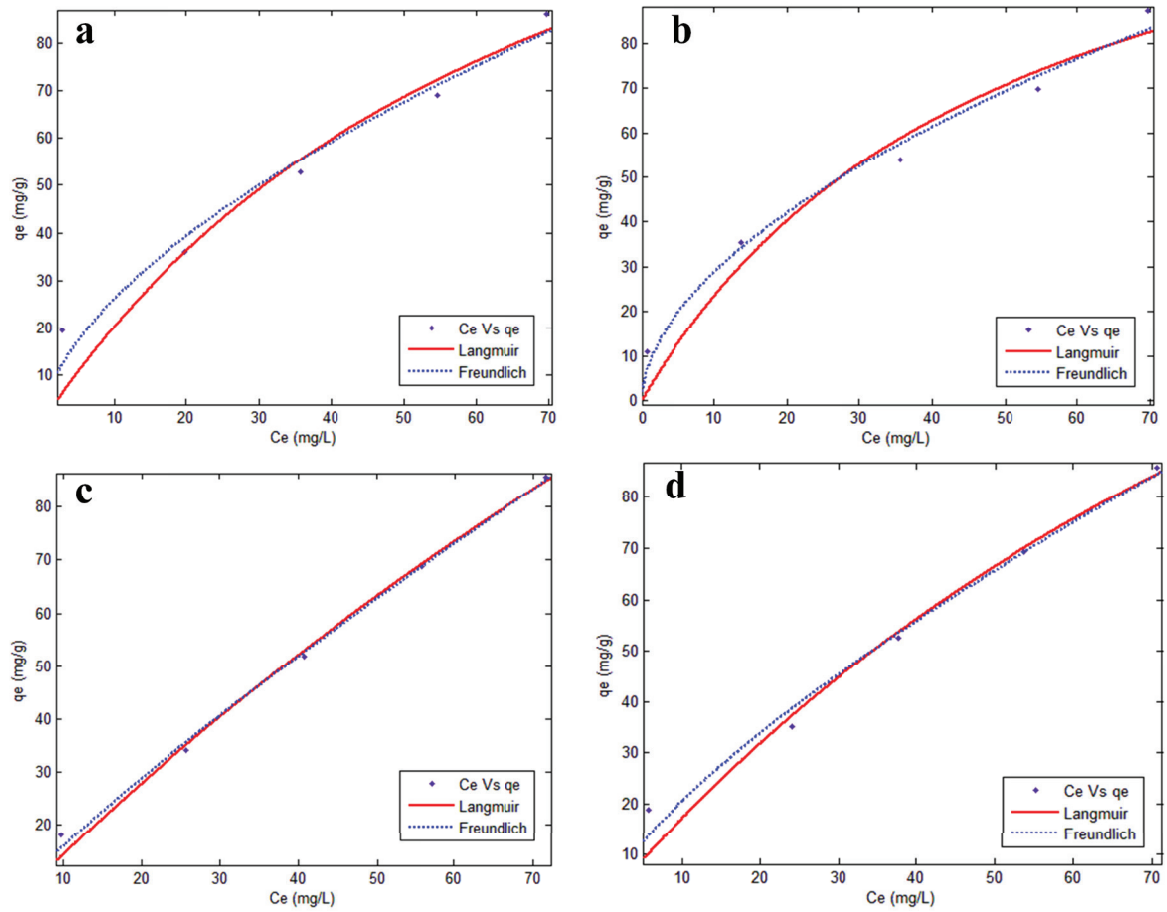

Fig. 7. Non-linear adsorption isotherm for adsorption of (a) Cu^{2+}, (b) Ni^{2+}, (c) Cd^{2+} and (d) Zn^{2+} ions onto PAC.

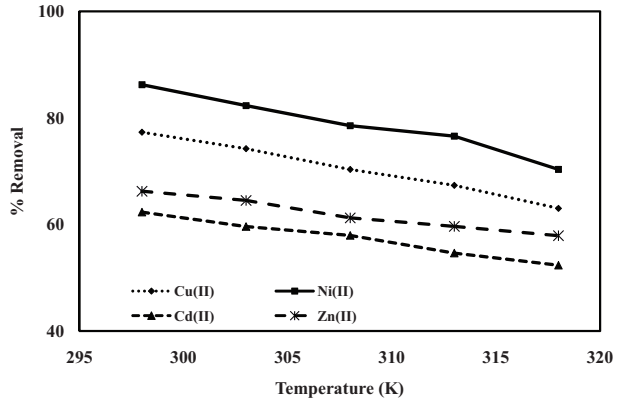

Fig. 8. Effect of temperature for the adsorption of metal ions onto PAC.

temperature, the interaction between metal ions and PAC surface is weaker than at lower temperature, which influenced the adsorption process and decreased adsorption nature. The negative ΔG° values indicate that the process is feasible and spontaneous in nature. The thermodynamic studies suggest that the PAC could be used as an adsorbent for the removal of divalent heavy metal ions in aqueous solution at the lower temperature and cannot be at a higher temperature.

3.6. Recyclability of PAC

Recyclability studies onto PAC were carried with 0.2 N HCl as an eluent and the results obtained are shown in Fig. 10. The adsorption–desorption cycles were repeated several times, and the desorption rate was found to be very rapid, as the almost highest desorption was noticed within 60 min, for the metal ions (Cu^{2+}, Ni^{2+}, Cd^{2+} and Zn^{2+} ions onto PAC). The recyclability results show that the efficiency of the recycled PAC for the removal of metal ions is nearly the same, as that of the fresh one, even after several cycles. The reasonable adsorption–desorption behavior of PAC makes it a good choice for multi-cyclic use. Based on this, it can be concluded that the PAC can serve as a better adsorbent for divalent metal ion removal from aqueous solution.

4. Conclusion

The use of the prepared PAC with various pore sizes for chelating toxic heavy metal ions by adsorption is a possible and an efficient method for solving the problem of the environmental pollution in aqueous media. The PAC is completely insoluble in aqueous media, and organic solvents and their stabilities can be controlled and received considerable attention in the removal of heavy metal ions owing to their inherent advantages over the other methods. The SEM morphological

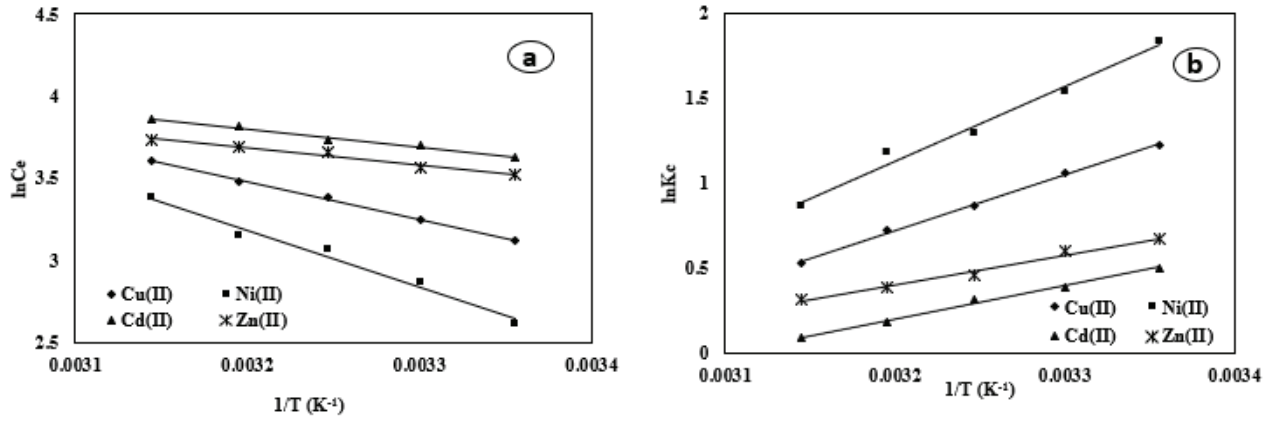

Fig. 9. (a) Plot of lnC_e against 1/T, (b) plot of lnK_c against 1/T for the adsorption of metal ions onto PAC.

Table 6
Thermodynamic parameters for the adsorption of Cu^{2+}, Ni^{2+}, Cd^{2+} and Zn^{2+} ions adsorption of PAC

Parameters	Temperature (°C)	Cu^{2+} ion	Ni^{2+} ion	Cd^{2+} ion	Zn^{2+} ion
R^2		0.998	0.983	0.992	0.985
$\Delta H°$(kJ mol)		392.1	523.7	232.8	209.7
$-\Delta S°$ (J/mol)		1.167	1.539	0.720	0.622
$-\Delta G°$ (kJ/mol)	298	3.307	1.179	0.360	0.349
	303	2.665	0.948	0.266	0.296
	308	2.208	0.758	0.209	0.220
	313	1.883	0.663	0.117	0.117
	318	1.409	0.452	0.054	0.138

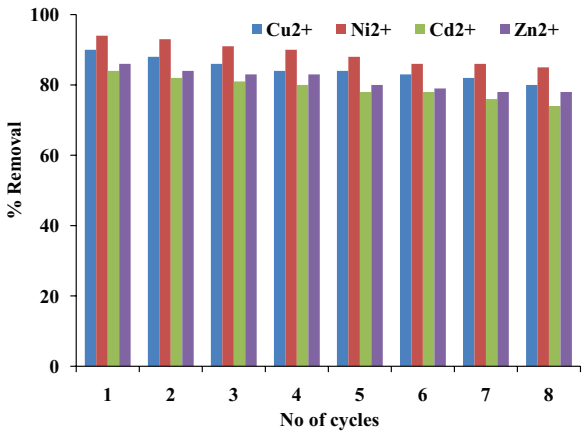

Fig. 10. Recyclability of Cu^{2+}, Ni^{2+}, Cd^{2+} and Zn^{2+} ions onto PAC.

study of PAC clearly indicates the presence of pores and cavities on the surface of the adsorbents which influence in the adsorption process. Adsorption parameters such as solution pH, adsorbent dosage, contact time and initial metal ions concentration were optimized. The competitive adsorption and selectivity results show that the PAC adsorbent has good adsorption selectivity and a high capacity for the removal of various metal ions from the mixture. The adsorption kinetic studies show that the calculated equilibrium adsorption capacity (q_e) values of the pseudo-second-order kinetic model agrees well with the experimental values. The adsorption isotherm studies show that the mono- and multi-layer adsorption process was occurring on the surface of PAC and the maximum monolayer adsorption capacities of PAC for Cu^{2+}, Ni^{2+}, Cd^{2+} and Zn^{2+} ions were calculated to be 69.50, 74.33, 54.61 and 60.32 mg/g, respectively. Studies on the effect of temperature showed that there is a decrease in the adsorption capacity (q_e) with an increase in temperature for PAC which reveals that they are endothermic in nature. The negative $\Delta G°$ values indicate that the process is feasible and spontaneous in nature. Based on the above observation, it could be concluded that PAC is a promising competent adsorbent for the removal of heavy metal ions from aqueous solutions, due to their high selectivity, thermal stability and absolute insolubility in water.

References

[1] A. Nieto-Marquez, A. Pinedo, G. Picasso, E. Atanes, R.S. Kou, Selective adsorption of Pb^{2+}, Cr^{3+} and Cd^{2+} mixtures on activated carbons prepared from waste tires, J. Environ. Chem. Eng., 5 (2017) 1060–1067.
[2] A. Murugesan, T. Vidhyadevi, S.S. Kalaivani, P. Baskaralingam, C.D. Anuradha, S. Sivanesan, Kinetic studies and isotherm modeling for the removal of Ni^{2+} and Pb^{2+} ions by modified activated carbon using sulfuric acid, Environ. Progr. Sustain. Energy, 33 (2013) 844–854.
[3] T. Vidhyadevi, A. Murugesan, S.S. Kalaivani, M. Anil Kumar, K.V. Thiruvenkada Ravi, L. Ravikumar, C.D. Anuradha, S. Sivanesan, Optimization of the process parameters for the

removal of reactive yellow dye by the low-cost *Setaria verticillata* carbon using Response surface methodology: thermodynamic, kinetic and equilibrium studies, Environ. Progr. Sustain. Energy, 33 (2013) 855–865.
[4] T. Vidhyadevi, A. Murugesan, S.S. Kalaivani, M.P. Premkumar, V. Vinoth Kumar, L. Ravikumar, S. Sivanesan, Evaluation of equilibrium, kinetic, and thermodynamic parameters for adsorption of Cd^{2+} ion and methyl red dye onto amorphous poly(azomethinethioamide) resin, Desal. Wat. Treat., 52 (2013) 3477–3488.
[5] P. Senthilkumar, C. Senthamarai, A. Durgadevi, Adsorption kinetics, mechanism, isotherm, and thermodynamic analysis of copper ions onto the surface modified agricultural waste, Environ. Progr. Sustain. Energy, 33 (2014) 28–37.
[6] E. Asuquo, A. Martin, P. Nzerem, F. Siperstein, X. Fan, Adsorption of Cd (II) and Pb (II) ions from aqueous solutions using mesoporous activated carbon adsorbent: equilibrium, kinetics and characterization studies, J. Environ. Chem. Eng., 5 (2016) 679–698.
[7] K. Anbalagan, P. Senthilkumar, R. Karthikeyan, Adsorption of toxic Cr(VI) ions from aqueous solution by sulphuric acid modified *Strychnos potatorum* seeds in batch and column studies, Desal. Wat. Treat., 57 (2016) 12585–12607.
[8] K. Anbalagan, P. Senthilkumar, K. Sangita Gayatri, S. Shahul Hameed, M. Sindhuja, C. Prabhakaran, R. Karthikeyan, Removal and recovery Ni(II) ions from synthetic wastewater using surface modified *Strychnos potatorum* seeds: experimental optimization and mechanism, Desal. Wat. Treat., 53 (2015) 171–182.
[9] H. Liu, B. Yang, N. Xue, Enhanced adsorption of benzene vapor on granular activated carbon under humid conditions due to shifts in hydrophobicity and total micropore volume, J. Hazard. Mater., 318 (2016) 425–432.
[10] K. Park, H. Nam, K.B. Lee, S. Mun, Adsorption behaviors of sugars and sulfuric acid on activated porous carbon, J. Ind. Eng. Chem., 34 (2016) 21–26.
[11] T. Yan, X. Luo, X. Lin, J. Yang, Preparation, characterization and adsorption properties for lead (II) of alkali-activated porous leather particles, Colloids Surf, A, 512 (2016) 7–16.
[12] G. Nagaraju, J. Lim, S. Cha, J. Yu, Three-dimensional activated porous carbon with meso/macropore structures derived from fallen pine cone flowers: a low-cost counter electrode material in dye-sensitized solar cells, J. Alloys Comp., 693 (2016) 1297–1304.
[13] U. Pearlin Kiruba, P. Senthilkumar, K. Sangita Gayatri, S. Shahul Hameed, M. Sindhuja, C. Prabhakaran, Study of adsorption kinetic, mechanism, isotherm, thermodynamic and design models for Cu(II) ions on sulphuric acid modified Eucalyptus seeds: temperature effect, Desal. Wat. Treat., 56 (2015) 2948–2965.
[14] A. Saravanan, P. Senthilkumar, B. Preetha, Optimization of process parameters for the removal of chromium(VI) and nickel(II) from aqueous solutions by mixed biosorbents (custard apple seeds and *Aspergillus niger*) using response surface methodology, Desal. Wat. Treat., 57 (2016) 14530–14543.
[15] S. Suganya, K. Kayalvizhi, P. Senthilkumar, A. Saravanan, V. Vinothkumar, Biosorption of Pb(II), Ni(II) and Cr(VI) ions from aqueous solution using *Rhizoclonium tortuosum*: extended application to nickel plating industrial wastewater, Desal. Wat. Treat., 57 (2016) 25114–25139.
[16] K. Nithya, Asha Sathish, P. SenthilKumar, T. Ramachandran, An insight into the prediction of biosorption mechanism, and isotherm, kinetic and thermodynamic studies for Ni(II) ions removal from aqueous solution using acid treated bio-sorbent: the *Lantana camara* fruit, Desal. Wat. Treat., 80 (2017) 276–287.
[17] H. Laksaci, A. Khelifi, B. Belhamdi, M. Trari, Valorization of coffee grounds into activated carbon using physic-chemical activation by KOH/CO_2, J. Environ. Chem. Eng., 5 (2017) 5061–5066.
[18] I. Quinones, G. Guiochon, Extension of a Jovanovic–Freundlich isotherm model to multicomponent adsorption on heterogeneous surfaces, J. Chromatogr. A, 796 (1998) 15–40.
[19] M. Chiou, G. Chuang, Competitive adsorption of dye metanil yellow and RB15 in acid solutions on chemically cross-linked chitosan beads, Chemosphere, 62 (2006) 731–740.
[20] D. Zhang, J. Yin, J. Zhao, H. Zhu, C. Wang, Adsorption and removal of tetracycline from water by petroleum coke-derived highly porous activated carbon, J. Environ. Chem. Eng., 3 (2015) 1504–1512.
[21] C. Ferreira Esmi, C. Guevar, M. Dhoury, L. Schrive, Y. Barre, J. Palmeri, A. Deratani, Evaluating the use of activated carbon felts to remove Co^{2+}, Ni^{2+} and Sr^{2+} from wastewater, J. Environ. Chem. Eng., 2 (2014) 1705–1712.
[22] Z. Zou, Y. Tang, C. Jiang, J. Zhang, Efficient adsorption of Cr(VI) on sunflower seed hull derived porous carbon, J. Environ. Chem. Eng., 3 (2015) 898–905.
[23] M.A. Devani, B. Munshi, J.U.K. Oubagaranadin, Characterization and use of chemically activated *Butea monosperma* leaf dust for mercury (II) removal from solutions, J. Environ. Chem. Eng., 3 (2015) 2212–2218.
[24] H. Tounsadi, A. Khalidi, A. Machrouhi, M. Farnane, R. Elmoubarki, A. Elhalil, M. Sadiq, N. Barka, Highly efficient activated carbon from *Glebionis coronaria* L. biomass: optimization of preparation conditions and heavy metals removal using experimental design approach, J. Environ. Chem. Eng., Part A, 4 (2016) 4549–4564.
[25] F. Sardella, M. Gimenez, C. Navas, C.a. Morandi, C. Deiana, K. Sapag, Conversion of viticultural industry wastes into activated carbons for removal of lead and cadmium, J. Environ. Chem. Eng., 3 (2015) 253–260.
[26] T. Naiya, A. Bhattacharyya, S. Das, Adsorptive removal of Cd(II) ions from aqueous solutions by rice husk ash, Environ. Progr. Sustain. Energy, 28 (2009) 535–546.
[27] O. Abdelwahab, Y. Fouad, N.K. Amin, H. Mandor, Kinetic and thermodynamic aspects of cadmium adsorption onto raw and activated guava (*Psidium guajava*) leaves, Environ. Progr. Sustain. Energy, 34 (2015) 351–358.
[28] E.D. Asuquo, A.D. Martin, Sorption of cadmium (II) ion from aqueous solution onto sweet potato (*Ipomoea batatas* L.) peel adsorbent: characterisation, kinetic and isotherm studies, J. Environ. Chem. Eng., 4 (2016) 4207–4228.
[29] R.M. Ali, H.A. Hamad, M.M. Hussein, G.F. Malash, Potential of using green adsorbent of heavy metal removal from aqueous solutions: adsorption kinetics, isotherm, thermodynamic, mechanism and economic analysis, Ecol. Eng., 91 (2106) 317–332.
[30] T. Naiya, A. Bhattacharyya, S. Das, Adsorption of Pb(II) by sawdust and neem bark from aqueous solutions, Environ. Progr. Sustain. Energy, 27 (2008) 313–328.
[31] G. Halder, S. Dhawane, P.K. Barai, A. Das, Optimizing chromium (VI) adsorption onto superheated steam activated granular carbon through response surface methodology and artificial neural network, Environ. Progr. Sustain. Energy, 34 (2015) 638–647.
[32] F. Hernainz, M. Calero, G. Blazquez, M.A. Martin-Lara, G. Tenorio, Comparative study of the biosorption of cadmium(II), chromium(III), and lead(II) by olive stone, Environ. Progr. Sustain. Energy, 27 (2008) 469–478.
[33] P. Senthilkumar, Adsorption of lead(II) ions from simulated wastewater using natural waste: a kinetic, thermodynamic and equilibrium study, Environ. Progr. Sustain. Energy, 33 (2014) 55–64.
[34] A. Murugesan, T. Vidhyadevi, S. DineshKirupha, L. Ravikumar, S. Sivanesan, Removal of chromium (VI) from aqueous solution using acid modified corncob activated carbon: equilibrium and kinetic studies, Environ. Progr. Sustain. Energy, 32 (2013) 673–680.
[35] S. Lagergren, About the theory of so-called adsorption of soluble substances, K. Sven. Vetensk.akad. Handl., 24 (1898) 1–39.
[36] Y.S. Ho, G. McKay, Pseudo-second order model for sorption processes, Process Biochem., 34 (1999) 451–465.
[37] Y.S. Ho, G. McKay, Application of kinetic models to the sorption of copper(II) onto peat, Adsorpt. Sci. Technol., 20 (2002) 797–815.

[38] F. Wu, R. Tseng, R. Juang, Characteristics of Elovich equation used for the analysis of adsorption kinetics in dye-chitosan systems, Chem. Eng. J., 150 (2002) 366–373.
[39] W.J. Weber, J.C. Morris, Kinetics of adsorption on carbon from solution, J. Sanit. Eng. Div. Am. Soc. Civ. Eng., 89 (1963) 31–60.
[40] I. Langmuir, The adsorption of gases on plane surfaces of glass, mica and platinum, J. Am. Chem. Soc., 40 (1918) 1361–1403.
[41] H.M.F. Freundlich, Over the adsorption in solution, J. Phys. Chem., 57 (1906) 385–470.
[42] A.A. Khan, R.P. Singh, Adsorption thermodynamics of carbofuran on Sn (IV) arsenosilicate in H^+, Na^+ and Ca^{2+} forms, Colloids Surf., 24 (1987) 33–42.
[43] A. Ramesh, D.J. Lee, J.W.C. Wong, Thermodynamic parameters for adsorption equilibrium of heavy metals and dyes from wastewater with low-cost adsorbents, J. Colloid Interface Sci., 291 (2005) 588–592.
[44] H. Chiu, J. Wang, Adsorption thermodynamics of cobalt ions onto attapulgite, J. Environ. Protect. Sci., 3 (2009) 102–106.
[45] D.M. Araujo-Melo, J.A. Ruiz, A.M. Melo, E.V. Sobrinho, A.V. Martinelli, Preparation and characterization of lanthanum palygorskite clays as acid catalysts, J. Alloys Comp., 344 (2002) 352–355.
[46] G.H. Pino, L.M.S. Mesquita, M.L. Torem, G.A.S. Pinto, Biosorption of cadmium by green coconut shell powder, Miner. Eng., 19 (2006) 380–387.
[47] W. Li, A. Zhao, P.R. Teasdale, R. John, S. Zhang, Synthesis and characterisation of a polyacrylamide-polyacrylic acid copolymer hydrogel for environmental analysis of Cu and Cd, React. Funct. Polym., 52 (2002) 31–41.
[48] G.A. Habeeb, M.M. Fayyadh, Rice husk ash concrete: the effect of RHA average particle size on mechanical properties and drying shrinkage, Aust. J. Basic Appl. Sci., 3 (2009) 1616–1622.
[49] H. Rehman, M. Shakirullah, I. Ahmad, S. Shah, Hamedullah. Sorption studies of nickel ions onto sawdust of *Dalbergia sissoo*, J. Chin. Chem. Soc., 53 (2006) 1045–1052.
[50] M.E. Argun, S. Dursun, C. Ozdemir, M. Karatas, Heavy metal adsorption by modified oak sawdust: thermodynamics and kinetics, J. Hazard. Mater., 141 (2007) 77–85.
[51] V.C. Taty-Costodes, H. Fauduet, C. Porte, A. Delacroix, Removal of Cd(II) and Pb(II) ions from aqueous solutions by adsorption onto sawdust of *Pinus sylvestris*, J. Hazard. Mater., 105 (2003) 121–142.
[52] S.R. Shukla, R.S. Pai, Adsorption of Cu(II), Ni(II) and Zn(II) on dye loaded groundnut shells and sawdust, Sep. Purif. Technol., 43 (2005) 1–8.
[53] Q. Li, J. Zhai, W. Zhang, M. Wang, J. Zhou, Kinetic studies of adsorption of Pb(II), Cr(III) and Cu(II) from aqueous solution by sawdust and modified peanut husk, J. Hazard. Mater., 141 (2006) 163–167.
[54] S.R. Shukla, R.S. Pai, Adsorption of Cu(II), Ni(II) and Zn(II) on modified jute fibres, Bioresour. Technol., 96 (2005) 1430–1438.
[55] K.S. Low, C.K. Lee, S.C. Liew, Sorption of cadmium and lead from aqueous solutions by spent grain, Process Biochem., 36 (2000) 59–64.
[56] Y.B. Onundi, A.A. Mamun, M.F. Al Khatib, Y.M. Ahmed, Adsorption of copper, nickel and lead ions from synthetic semiconductor industrial wastewater by palm shell activated carbon, Int. J. Environ. Sci. Technol., 7 (2010) 751–758.
[57] T. Bohli, A. Ouederni, N. Fiol, I. Villaescusa, Uptake of Cd^{2+} and Ni^{2+} metal ions from aqueous solutions by activated carbons derived from waste olive stones, Int. J. Chem. Eng. Appl., 3 (2012) 232–236.
[58] H. Hasar, Adsorption of nickel(II) from aqueous solution onto activated carbon prepared from almond husk, J. Hazard. Mater., B97 (2003) 49–57.

Supplementary figures

Fig. S1. Image of punnai shells.

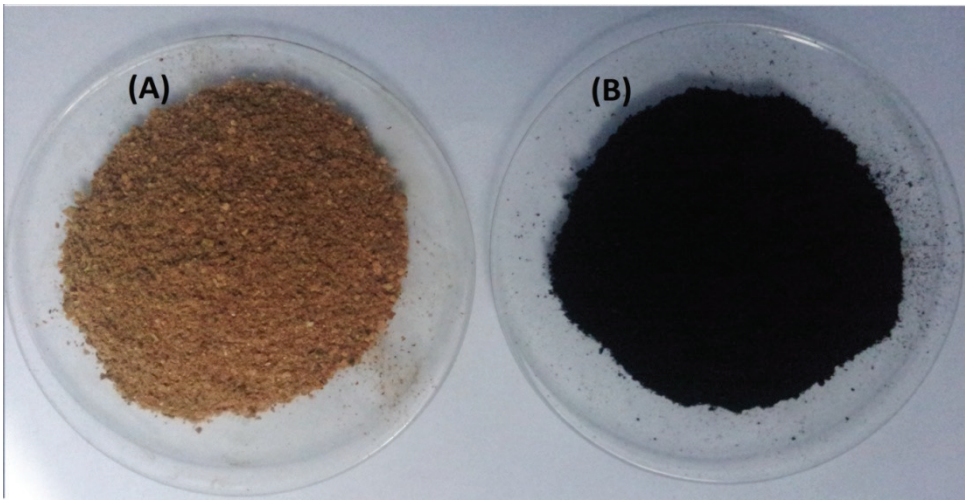

Fig. S2. (A) Raw material and (B) acid-enhanced activated carbons of punnai shells.